Functional Convergence of Developmentally and Adult-Generated Granule Cells in Dentate Gyrus Circuits Supporting Hippocampus-Dependent Memory

Scellig S.D. Stone,[1,2,3,4] Cátia M. Teixeira,[1,5] Kirill Zaslavsky,[1] Anne L. Wheeler,[1,2] Alonso Martinez-Canabal,[1,2] Afra H. Wang,[1,2] Masanori Sakaguchi,[1] Andres M. Lozano,[2,3,4] and Paul W. Frankland[1,2,6]*

ABSTRACT: In the hippocampus, the production of dentate granule cells (DGCs) persists into adulthood. As adult-generated neurons are thought to contribute to hippocampal memory processing, promoting adult neurogenesis therefore offers the potential for restoring mnemonic function in the aged or diseased brain. Within this regenerative context, one key issue is whether developmentally generated and adult-generated DGCs represent functionally equivalent or distinct neuronal populations. To address this, we labeled separate cohorts of developmentally generated and adult-generated DGCs and used immunohistochemical approaches to compare their integration into circuits supporting hippocampus-dependent memory in intact mice. First, in the water maze task, rates of integration of adult-generated DGCs were regulated by maturation, with maximal integration not occurring until DGCs were five or more weeks in age. Second, these rates of integration were equivalent for embryonically, postnatally, and adult-generated DGCs. Third, these findings generalized to another hippocampus-dependent task, contextual fear conditioning. Together, these experiments indicate that developmentally generated and adult-generated DGCs are integrated into hippocampal memory networks at similar rates, and suggest a functional equivalence between DGCs generated at different developmental stages. © **2010 Wiley-Liss, Inc.**

KEY WORDS: neurogenesis; contextual fear con- ditioning; Morris water maze; learning; mice

[1] **Program in Neurosciences and Mental Health, The Hospital for Sick Children, Toronto, Ontario, Canada M5G 1X8;** [2] **Institute of Medical Science, University of Toronto, Toronto, Ontario, Canada, M5S 1A8;** [3] **Division of Neurosurgery, Department of Surgery, University of Toronto, Toronto, Ontario, Canada, M5G 1X8;** [4] **Division of Neurosurgery, Toronto Western Hospital, University Health Network, Toronto, Ontario, Canada, M5T 2S8;** [5] **Graduate Program in Areas of Basic and Applied Biology (GABBA), Universidade do Porto, 4050-465 Porto, Portugal;** [6] **Department of Physiology, University of Toronto, Toronto, Ontario, Canada, M5S 1A8**

Additional Supporting Information may be found in the online version of this article.

Scellig S.D. Stone and Cátia M. Teixeira contributed equally to this work.

Grant sponsor: Canadian Institutes of Health Research; Grant number: MOP-86762, EJLB Foundation; Fellowship grant sponsors: CIHR Research fellowship, the Department of Surgery's Surgeon Scientist Program at the University of Toronto, Graduate Program in Areas of Basic and Applied Biology (GABBA), the Portuguese Foundation for Science and Technology (FCT), Ontario Mental Health Foundation, El Consejo Nacional de Ciencia y Tecnologia (Mexico), the Hospital for Sick Children, Japanese Society for the Promotion of Science Postdoctoral Fellowship Program.

*Correspondence to: Paul W. Frankland, Neurosciences and Mental Health, The Hospital for Sick Children, 555 University Ave., 6018 McMaster Building, Toronto, Ontario, Canada, M5G 1X8.
E-mail: paul.frankland@sickkids.ca

Accepted for publication 8 June 2010
DOI 10.1002/hipo.20845
Published online in Wiley Online Library (wileyonlinelibrary.com).

INTRODUCTION

During adulthood, new neurons are continuously added to the dentate gyrus (DG), a subregion of the hippocampus that plays an essential role in memory formation (Ming and Song, 2005; Zhao et al., 2008). Similar to developmentally generated DGCs, these adult-generated DGCs are thought to eventually contribute to the formation of hippocampus-dependent memory (Shors, 2008; Deng et al., 2009a,b). One key question for understanding how these adult-generated DGCs contribute to memory function is whether they are functionally distinct from DGCs generated during development. While adult-generated DGCs may eventually develop similar cellular phenotypes to developmentally generated DGCs (Laplagne et al., 2006, 2007), adult-generated DGCs differ transiently from their developmentally generated neighbors. For example, between two and four weeks of age the threshold for long-term potentiation (LTP) is reduced (Schmidt-Hieber et al., 2004; Ge et al., 2007), and from four to six weeks LTP magnitude is increased (Ge et al., 2007). In particular, these transient changes in the threshold and magnitude of LTP may promote integration of newborn neurons into hippocampal memory networks by allowing them to either temporarily or permanently out-compete their developmentally generated neighbors. Such a competitive mechanism has been proposed to allow the DG to temporally associate event memories that occur close together in time (Aimone et al., 2006, 2009). Alternatively, developmentally generated and adult-generated DGCs may be functionally equivalent. According to this view, developmentally generated and adult-generated DGCs would be integrated into hippocampal memory circuits at equivalent rates.

Previously this question has been addressed using immunohistochemical approaches to estimate integration rates of DGCs into hippocampal memory networks in intact mice (Ramirez-Amaya et al., 2006; Kee et al., 2007a,b; Tashiro et al., 2007). In these studies, proliferation markers such as BrdU were used to label adult-generated DGCs. Typically, mice were then trained in a hippocampus-dependent task (such

as the hidden platform version of the water maze), and expression of immediate early genes (IEGs; such as *c-fos*, *Arc*, *zif268*) quantified following memory testing. Because IEG expression is regulated by neuronal activity (Guzowski et al., 2005), this approach makes it possible to estimate the proportion of adult-generated DGCs that have been integrated into hippocampal memory networks by calculating the likelihood of IEG expression in BrdU+ cells. Integration rates of developmentally-generated DGCs can then be estimated by calculating the likelihood of IEG expression in cells expressing the neuronal marker NeuN. However, NeuN is expressed in cells as young as three-days-old (Brandt et al., 2003) and adult-generated DGCs <2-weeks-old do not express Fos (Jessberger and Kempermann, 2003). Therefore, these analyses likely underestimate recruitment rates for developmentally generated cells, and potentially lead to the impression that adult-generated DGCs are integrated at preferential rates. To circumvent this issue, in the current study we chose to directly label separate cohorts of embryonically, postnatally, and adult-generated DGCs by injecting different thymidine analogs (BrdU, IdU, CldU) at different developmental stages, and compare their rates of integration by quantifying IEG expression.

MATERIALS AND METHODS

Mice

Male offspring from a cross between C57Bl/6NTacfBr [C57B6] and 129Svev [129] mice (Taconic, Germantown, NY) were used in these experiments. All mice were bred in our colony at The Hospital for Sick Children, and maintained on a 12 h light/dark cycle with free access to food and water. Behavioral procedures were conducted during the light phase of the cycle, blind to the treatment condition of the mouse and according to protocols approved by the Animal Care Committee at The Hospital for Sick Children.

Water Maze Apparatus and Procedures

The apparatus and behavioral procedures have been previously described (Teixeira et al., 2006). Behavioral testing was conducted in a circular water maze tank (120 cm in diameter, 50 cm deep), located in a dimly-lit room. The pool was filled to a depth of 40 cm with water made opaque by adding white, non-toxic paint. Water temperature was maintained at 28 ± 1°C by a heating pad beneath the pool. A circular escape platform (10 cm diameter) was submerged 0.5 cm below the water surface, in a fixed position in one quadrant. The pool was surrounded by curtains, at least 1 m from the perimeter of the pool. The curtains were white with distinct cues painted on them.

Prior to commencing training, mice were individually handled for 2 min each day over seven consecutive days. Mice were trained over five days. On each training day, mice received six training trials (presented in two blocks of three trials; inter-block interval was ~1 h, intertrial interval was ~15 s). On each trial they were placed into the pool, facing the wall, in one of four start locations. The order of these start locations was pseudorandomly varied throughout training. The trial was complete once the mouse found the platform or 60 s had elapsed. If the mouse failed to find the platform on a given trial, the experimenter guided the mouse onto the platform. Following the completion of training, spatial memory was assessed in a series of three probe tests with an intertest interval of ~3 min. In this test the platform was removed from the pool, and the mouse was allowed 60 s to search for it.

Behavioral data from training and the probe tests were acquired and analyzed using an automated tracking system (Actimetrics, Wilmette, IL). In probe tests we quantified performance in two ways. First, we measured the amount of time mice searched the target zone (20 cm radius, centered on the location of the platform during training) vs. the average of three other equivalent zones in other areas of the pool. These zones each represent approximately 11% of the total pool surface. Second, we represented probe test performance as a heat map (or density plot), with hot colors corresponding to areas of the pool that were more frequently visited.

Contextual Fear Conditioning Apparatus and Procedures

The apparatus and behavioral procedures have been previously described (Wang et al., 2009). Contextual fear conditioning experiments were conducted in a windowless room containing four conditioning chambers. Each conditioning context consisted of a stainless steel conditioning chamber (31 cm × 24 cm × 21 cm; Med Associates, St. Albans, VT), containing a stainless steel shock-grid floor. Shock grid bars (diameter 3.2 mm) were spaced 7.9 mm apart. The grid floor was positioned over a stainless-steel drop-pan, which was lightly cleaned with 70% ethyl alcohol to provide a background odor. The front, top, and back of the chamber were made of clear acrylic and the two sides made of modular aluminum. Mouse freezing behavior was monitored via four overhead cameras. Freezing was assessed using an automated scoring system (Actimetrics, Wilmette, IL), which digitized the video signal at 4 Hz and compared movement frame by frame to determine the amount of freezing.

During training, mice were placed in the context for 5 min and were presented with 3 unsignaled footshocks (0.5 mA, 2 s, 1 min apart) starting at 2 min. Following the last footshock mice remained in the context for an additional minute, and then were returned to their home cage. On the test day, mice were placed back into the same context for a total of 5 min and freezing was monitored.

PTZ Treatment

Mice were initially injected intraperitoneally (i.p.) with 30 mg/kg of the chemical convulsant Pentylenetetrazole (PTZ; Sigma, MO) followed by additional 10 mg/kg injections every

15 min as needed. This procedure was repeated until a seizure occurred, typically requiring a total dose of 60 mg/kg.

Entorhinal Cortex Electrical Stimulation

Mice were pre-treated with atropine sulfate (0.1 mg/kg, i.p.), anesthetized with chloral hydrate (400 mg/kg, i.p.) and placed in a stereotaxic frame. The scalp was incised and a hole drilled in the skull above the lateral entorhinal cortex (EC) [AP = −4.0 mm, ML = 3.3 mm relative to bregma] (Paxinos and Franklin, 2000). A concentric bipolar stimulating electrode (FHC Inc., Bowdoin, ME) was inserted to 5.0 mm below bregma into the lateral EC (Paxinos and Franklin, 2000), and high-frequencey electrical stimulation (130 Hz, 90 μs pw, 50 μA) was delivered using a Medtronic 3628 screener (Medtronic Inc., Minneapolis, MN) for 1 h. At the completion of surgery, animals were kept anesthetized until sacrifice.

BrdU, CldU, and IdU Administration

5-bromo-2′-deoxyuridine (BrdU; Sigma, St. Louis, MO) was dissolved in 0.1 M phosphate-buffered saline (PBS) and heated to 50–60°C, at a concentration of 10 mg/ml. In experiments 2, 3, 6, and 7, animals received 50 mg/kg of BrdU per injection either i.p. on postnatal Day 7 (P7) or 60 (P60), or subcutaneously (s.c.) around gestational Day 18 (E18). Exposure to even higher doses of BrdU at these embryonic and postnatal stages of development does not impact number, development or behavior of progeny (Kolb et al., 1999; Vega and Peterson, 2005; Bick-Sander et al., 2006).

5-Iodo-2′-deoxyuridine (IdU; MP Biomedicals, Solon, OH) or 5-Chloro-2′-deoxyuridine (CldU; Sigma, MO) (IdU and CldU are collectively referred to as XdU) were dissolved in 0.1 M PBS and heated to 50–60°C, at a concentration of 10 mg/ml. In Experiments 4 and 5, animals received the same molar concentration of XdU as 50 mg/kg of BrdU per injection either i.p. on P7 or P60, or s.c. around E18. Actual equimolar doses used were 57.5 mg/kg of IdU, and 42.5 mg/kg of CldU per injection.

Experimental Methods

Experiment 1 (Fig. 1) evaluated the activity-dependent regulation of Fos, and coexpression of Fos and Arc, in DGCs. Fos expression was assessed in the home cage (HC) condition (n = 3), following memory recall (n = 3) and after PTZ-induced seizures (n = 3) in 8 week old mice. Mice analyzed following memory recall underwent water maze training followed by a probe test one day later. Age-matched HC animals were sacrificed simultaneously. Fos expression was also examined in mice receiving high frequency EC electrical stimulation (n = 6), electrode-implanted but nonstimulated mice (n = 8) and age-matched HC animals (n = 4). Finally, Fos and Arc expression in DGCs was examined in adult mice (n = 4) that were trained and then tested one day later.

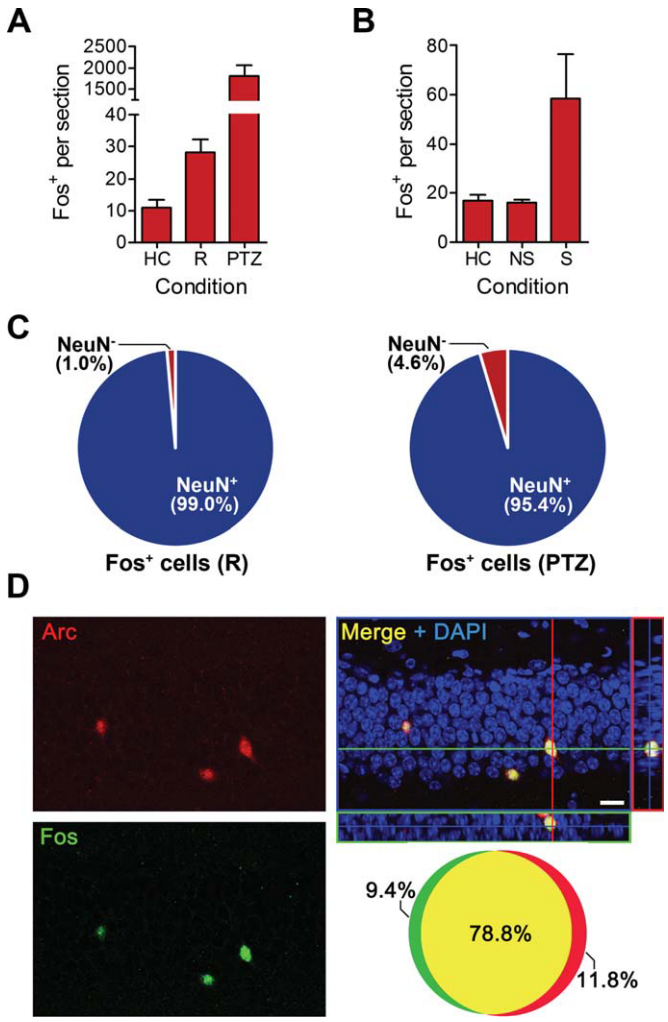

FIGURE 1. Activity-dependent regulation of Fos in DGCs. A: Induction of Fos in DGCs following spatial memory recall (R) and PTZ treatment compared to home cage (HC) mice. These and all subsequent graphs show mean number of cells per DG section ± SEM. B: Induction of Fos in dentate gyrus cells following stimulation (S) of the lateral entorhinal cortex compared to non-stimulated (NS) and home cage (HC) control mice. C: Left, the proportion of Fos+ dentate gyrus cells that were NeuN+ (a neuronal specific marker) following memory recall (R). Right, the proportion of Fos+ dentate gyrus cells that were NeuN+ following PTZ treatment (PTZ). D: Representative confocal images of Fos+, Arc+ and Fos+/Arc+ (merge) cells in the DG following behavioral testing (scale bar = 10 μm). Venn diagram of Fos+ (green) and Arc+ (red) DGCs, indicating that Fos and Arc were almost always colocalized (yellow) in the same DGCs. [Color figure can be viewed in the online issue, which is available at wileyonlinelibrary.com.]

Experiment 2 (Fig. 2) determined the age at which adult-generated DGCs are incorporated into spatial memory networks. To label dividing cells, 8-week-old mice were injected with BrdU (two injections/day, ∼12 h apart, for five days). Separate groups were then trained in the water maze either one week (n = 8), five weeks (n = 18), 7.5 weeks (n = 18), or 10 weeks (n = 18) later. Spatial memory was assessed one day following the completion of training. To control for cell age, an

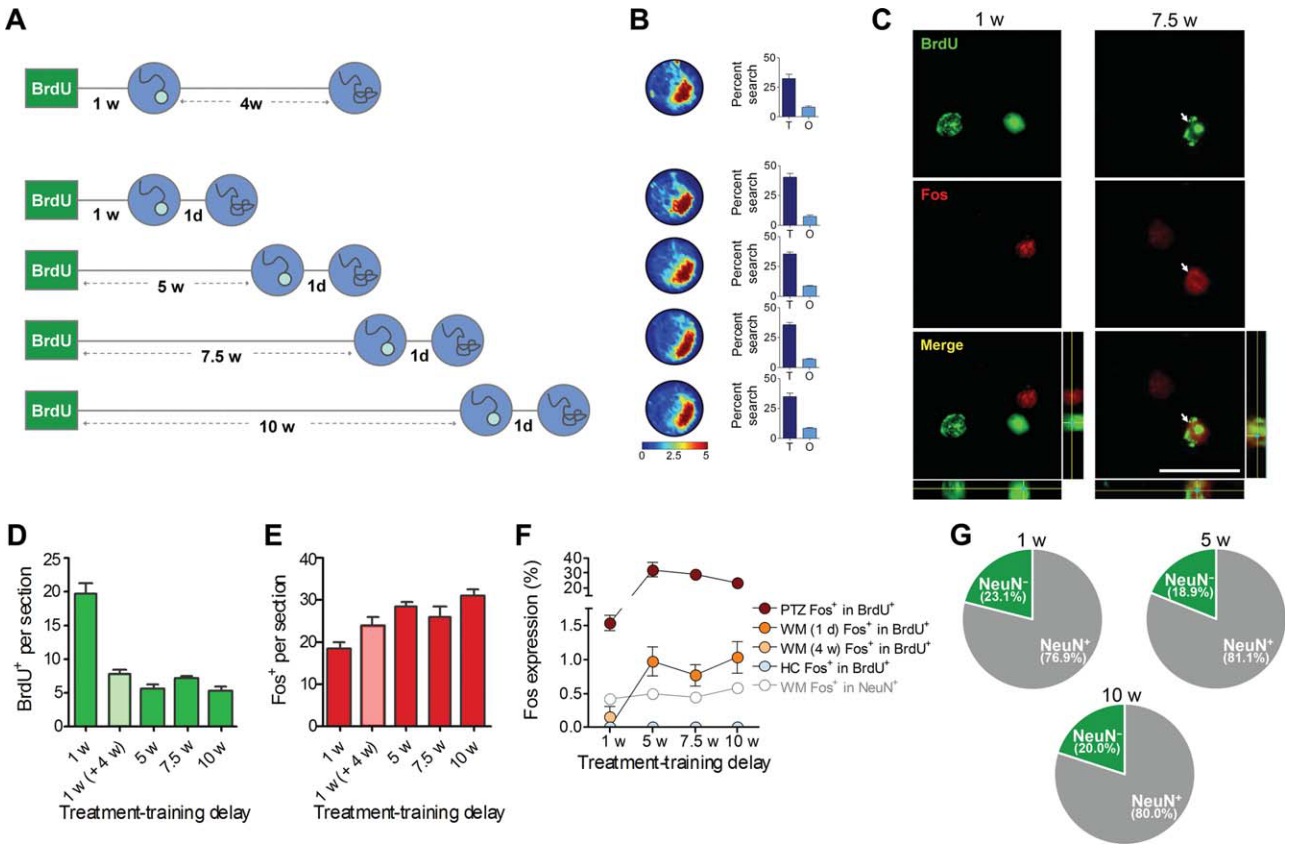

FIGURE 2. Maturation regulates adult-generated DGC integration into hippocampal circuits supporting water maze memory. A: Experimental design. B: Mice searched selectively in each of the three probe tests. In this and subsequent figures, only data from the first probe test are shown. Left, density plots for grouped data showing where mice concentrated their searches. The color scale represents the number of visits per animal per 5 cm × 5 cm area. Right, all groups of mice spent more time searching the target zone (T) compared with other (O) zones. C: Representative confocal images of BrdU+, Fos+ and Fos+/BrdU+ (arrow) cells in the DG following water maze testing in the 1-week and 7.5-week groups (scale bar = 20 μm). D: Numbers of BrdU+ cells in the DG. (E) Fos+ cells in the DG following probe tests. (F) Fos expression in BrdU+ cells (orange) or NeuN+ cells (clear). Fos in BrdU+ cells increased with longer delays between BrdU treatment and water maze training. Fos expression in matched BrdU-treated mice is shown following PTZ treatment (red) or in a home cage condition (light blue). (G) Proportion of BrdU+ cells that are NeuN+ in the GCL 1, 5 or 10 weeks after BrdU treatment. [Color figure can be viewed in the online issue, which is available at wileyonlinelibrary.com.]

additional group of mice (n = 10) were trained one week following BrdU treatment and then tested four weeks later. Further groups were treated with PTZ. Injections occurred either one week (n = 2), five weeks (n = 3), 7.5 weeks (n = 3), or 10 weeks (n = 3) after BrdU treatment. Age-matched HC groups were sacrificed at the same time as the one week (n = 3), five weeks (n = 3), 7.5 weeks (n = 3), and 10 weeks (n = 3) post BrdU treatment groups.

Experiment 3 (Fig. 3) compared recruitment rates of embryonically, postnatally, and adult-generated DGCs into spatial networks in the DG, controlling for cell age. BrdU was administered to pregnant mothers once around E18 (n = 6), mouse pups once at P7 (n = 6) or adult mice at P60 (two injections/day, ~12 h apart, for five days) (n = 18). All groups were then trained 7.5 weeks later and spatial memory was tested one day following the completion of training. Additional groups were first treated with equivalent doses of BrdU at E18 (n = 3), P7 (n = 3) or P60 (n = 3), and then treated with PTZ. PTZ injections occurred 7.5 weeks following BrdU treatment, matching the age at which water maze animals underwent training and testing.

Experiment 4 (Fig. 4) tested the sensitivity and specificity of CldU and IdU cell-labeling. One group of mice was treated with CldU once at P7, and then IdU at P60 (2 injections/day, ~12 h apart, for five days) (n = 3). A second group received IdU once at P7, followed by CldU (two injections/day, ~12 h apart, for five days) (n = 4). A third group of mice received both CldU and IdU simultaneously for two days (n = 3) at P60. All groups were sacrificed one day following the completion of injections.

Experiment 5 (Fig. 5) compared recruitment rates of embryonically, postnatally, and adult-generated DGCs into spatial memory networks in the same mouse. In the first group, pregnant mothers were treated with CldU once at E18, and then progeny (n = 12), were treated with IdU at P60 (two injections/day, ~12 h apart, for five days). In the second group (n = 14), mice were treated once with CldU at P7, and then with IdU at P60 (two injections/day, ~12 h apart, for five

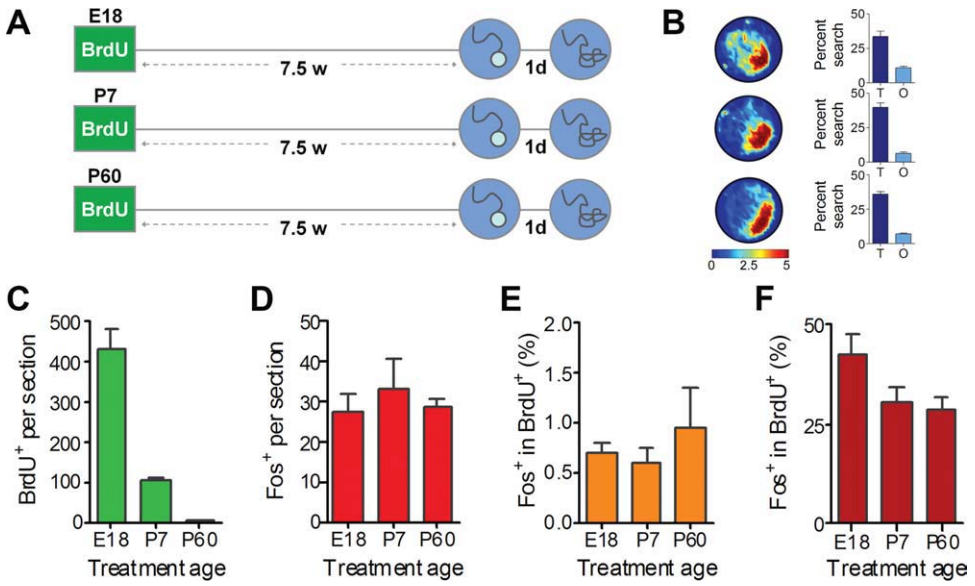

FIGURE 3. Integration of equivalently-aged E18, P7 and P60 DGCs. A: Experimental design. Separate groups of mice were treated with BrdU at E18, P7, and P60 and then trained in the water maze 7.5 weeks later. Spatial memory was tested in a series of three probe tests one day following the completion of training. B: Mice searched selectively in the probe tests. Left, density plots for grouped data showing where mice concentrated their searches. The color scale represents the number of visits per animal per 5 cm × 5 cm area. Right, all groups of mice spent more time searching the target zone (T) compared with other (O) zones. C: Number of BrdU+ cells was highest in the E18 group, followed by P7, and then P60, reflecting higher rates of developmental neurogenesis. D: Equivalent Fos expression in the DG across groups following probe tests. E: The likelihood of Fos expression in BrdU+ cells following probe tests was similar in all groups, suggesting that developmentally and adult-generated cells are integrated into DG circuits supporting water maze memory at similar rates. F: Fos expression in matched BrdU-treated mice is shown following PTZ treatment. [Color figure can be viewed in the online issue, which is available at wileyonlinelibrary.com.]

days). Both groups were trained in the water maze 7.5 weeks after IdU treatment, and spatial memory was assessed one day following the completion of training.

Experiment 6 (Fig. 6) evaluated the influence of cell age on integration of adult-generated DGCs into hippocampal networks supporting contextual fear memory. Mice were initially injected with BrdU (two injections/day, ~12 h apart, for five days), and separate groups were trained in the contextual fear conditioning task either one week (n = 10) or six weeks (n = 18) later. Contextual fear memory was assessed in all mice four weeks following training. In addition, Fos expression in BrdU+ cells was examined in HC control mice and mice treated with PTZ either 5 (HC, n = 3; PTZ, n = 2) or 10 (HC, n = 6; PTZ, n = 3) weeks following BrdU treatment.

Experiment 7 (Fig. 7) compared recruitment rates of developmentally and adult-generated DGCs into contextual fear memory networks in the DG. One group of mice (n = 6) was treated with BrdU once at P7 and then trained at P100. A second group (n = 27) was treated with BrdU (two injections/day, ~12 h apart, for five days) at P60, and then trained at P100. Contextual fear memory was assessed in both groups four weeks after training.

Tissue Handling and Preparation for Stereology

Ninety min following the completion of behavioral testing, PTZ-induced seizure activity or EC stimulation, mice were anesthetized and perfused transcardially with PBS and then 4% paraformaldehyde (PFA). Brains were removed, fixed overnight in PFA and then transferred to 30% sucrose solution (PBS for Fos/Arc colabeling, Experiment 1) and stored at 4°C. 50 m coronal cryostat sections (vibratome sections for Fos/Arc colabeling, Experiment 1) were cut beginning from a random starting point and continuing along the entire anterior-posterior extent of the DG. Sections were kept in sequential order and maintained free-floating in PBS. A 1/4 section sampling fraction was used to create four sets (each containing sections at 200-μm intervals) for use in immunohistochemical staining. Accordingly, each set comprised a systematic random sample representative of the entire DG for use in quantification analyses. Additional sets were stored in a PBS solution containing 0.02% sodium azide for later processing.

Immunohistochemistry

For Fos/Arc double labeling, sections were treated with 1% hydrogen peroxide (Sigma-Aldrich, St. Louis, MO) and ice-cold acetone (Sigma-Aldrich, St. Louis, MO). A rabbit on rabbit staining technique was employed, beginning by incubating sections with 70 ng/ml (1:15,000) of rabbit anti-Arc polyclonal antibody (Synaptic Systems, Goettingen, Germany). Arc protein was visualized using biotin conjugated donkey anti-rabbit antibody (1:500; Jackson Immunoresearch, West Grove, PA), avidin-biotin-peroxidase complex (Vector laboratories, Burlin-

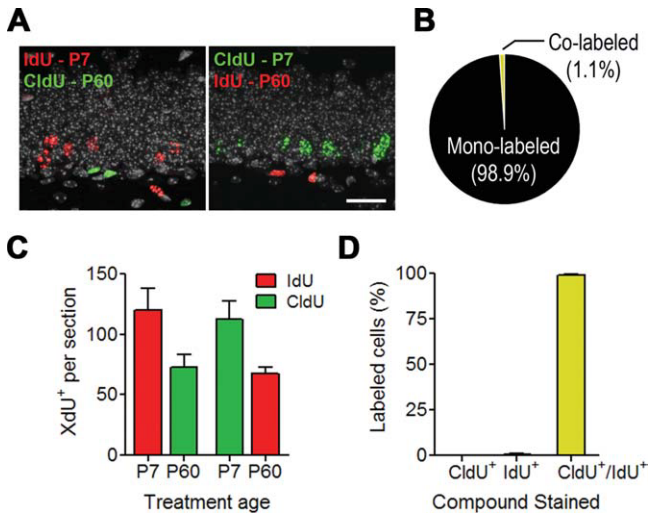

FIGURE 4. Sensitivity and specificity of CldU and IdU cell labeling and staining. A: Representative images of DGCs labeled by IdU injection at P7 and CldU injections at P60 (left), or CldU injection at P7 and IdU injections at P60 (right) (DAPI counterstain, scale bar = 20 μm). B: Proportions of CldU- and IdU-labeled DGCs that were colabeled vs. mono-labeled for CldU and/or IdU. C: Regardless of whether IdU or CldU was administered at P7, similar numbers of DGCs were labeled. Likewise, regardless of whether IdU or CldU was administered at P60, similar numbers of DGCs were labeled. D: Proportions of adult-labeled DGCs that were mono-labeled CldU+ or IdU+, or colabeled for both, following simultaneous injections of equimolar CldU and IdU at P60. [Color figure can be viewed in the online issue, which is available at wileyonlinelibrary.com.]

game, CA), tyramide signal amplification (made by mixing biotin succcinimidyl ester (Sigma-Aldrich, St. Louis, MO) and tyramine HCL (Fluka, St. Louis, MO)) and Alexa-568 conjugated streptavidin (1:500; Invitrogen, Carlsbad, CA). Next, residual rabbit IgG epitopes were blocked with donkey anti-rabbit IgG monovalent antibody (1:500; Jackson Immunoresearch, West Grove, PA). Fos protein was visualized using rabbit anticFos polyclonal antibody (1:1,500; Calbiochem, San Diego, CA) and Alexa-488 conjugated antirabbit antibody (1:500; Invitrogen, Carlsbad, CA). To rule out cross-reactivity between the Alexa-488 conjugated antirabbit and rabbit anti-Arc antibodies, we carried out staining without anticFos antibody and confirmed the absence of a Fos signal.

For BrdU/Fos staining, the BrdU antigen was exposed by incubating the sections in 1 N HCl at 45°C for 30 min. Incubation for 48 h at 4°C was performed using primary antibodies against Fos (rabbit anti-Fos polyclonal antibody; 1:1,000; Calbiochem, San Diego, CA) and BrdU (rat anti-BrdU monoclonal antibody; 1:500; Accurate Chemicals, Westbury, NY). Secondary antibody staining with Alexa-488 goat anti-rat and Alexa-568 goat anti-rabbit (1:500; Molecular Probes, Eugene, OR) was carried out for 2 h at room temperature. Antibodies were diluted in blocking solution containing 2% goat serum, 1% bovine serum albumin, and 0.2% Triton X-100 dissolved in PBS. Sections were mounted on slides (VWR, West Chester, PA) with Permafluor anti-fade medium (Lipshaw Immunon, Pittsburgh, PA).

For BrdU/neuronal-specific nuclear protein (NeuN) double labeling, identical procedures were performed while exchanging anti-Fos primary and antirabbit secondary antibodies with mouse anti-NeuN (1:1,000; Chemicon, Temecula, CA) and Alexa-568 goat antimouse (1:500; Molecular Probes, Eugene, OR), respectively.

For BrdU/Fos/NeuN triple labeling, identical procedures were performed using primary rabbit anti-Fos, rat anti-BrdU and mouse anti-NeuN antibodies. As secondary antibodies we used Alexa-488 goat antirat, Alexa-568 goat antimouse and Biotin-SP- conjugated antirabbit (1:500; Jackson ImmunoResearch, West Grove, PA). Biotin-SP-conjugated antirabbit primary antibody was detected by subsequent incubation with cy5 conjugated streptavidin (Zymed, San Francisco, CA).

For XdU/Fos staining, sections were washed with tris-buffered saline (TBS) followed by DNA denaturation in 1N HCl at 45°C for 30 min. Following additional washes with TBS, sections were incubated in primary antibodies: mouse anti-BrdU monoclonal antibody (BD Biosciences, San Jose, CA) at 1:1,000 for IdU, rat anti-BrdU monoclonal antibody (Accurate Chemicals, Westbury, NY) at 1:500 for CldU, and rabbit anti-Fos polyclonal antibody (Calbiochem, San Diego, CA) at 1:1,000 for 48 h at 4°C. After three washes in 3x TBS-tween 20, sections were incubated for 2 h at room temperature in secondary antibodies: Rhodamine Red-X-conjugated antimouse, FITC-conjugated antirat and Biotin-SP-conjugated antirabbit (Jackson ImmunoResearch, West Grove, PA). Subsequent to three washes with 3× PBS, biotinylated secondary antibody was detected with cy5 conjugated streptavidin (1:50; Zymed, San Francisco, CA).

For XdU/NeuN staining, identical procedures were performed except sections were first stained with XdU primary and secondary antibodies alone, replacing FITC-conjugated antirat secondary with biotinylated goat antirat (Vector Laboratories, Burlingame, CA) followed by cy5 conjugated streptavidin (Zymed, San Francisco, CA). At the completion of XdU staining, sections were incubated for 2 h at room temperature with Alexa-488 mouse anti-NeuN (1:1,000, Chemicon, Temecula, CA).

Imaging

Data and images were acquired using either a Nikon Eclipse 80i or Olympus BX61 epifluorescent microscope, or an Olympus IX81 with DSU or Zeiss LSM710 confocal microscope. Analysis for cell counting used Image J software (National Institute of Health, Bethesda, MD), and for spatial measurements and confocal examination used Image-Pro 6.2 software (Media Cybernetics Inc., Bethesda, MD) or ZEN 2009 software (Zeiss, Oberkochen, Germany).

Stereologic Quantification of Cells

Total cell counts obtained from a 1/4 systematic random section sampling fraction covering the entire anterior-posterior extent of the DG were divided by the total number of DG sections analyzed. Thus, normalized values for the number of cells

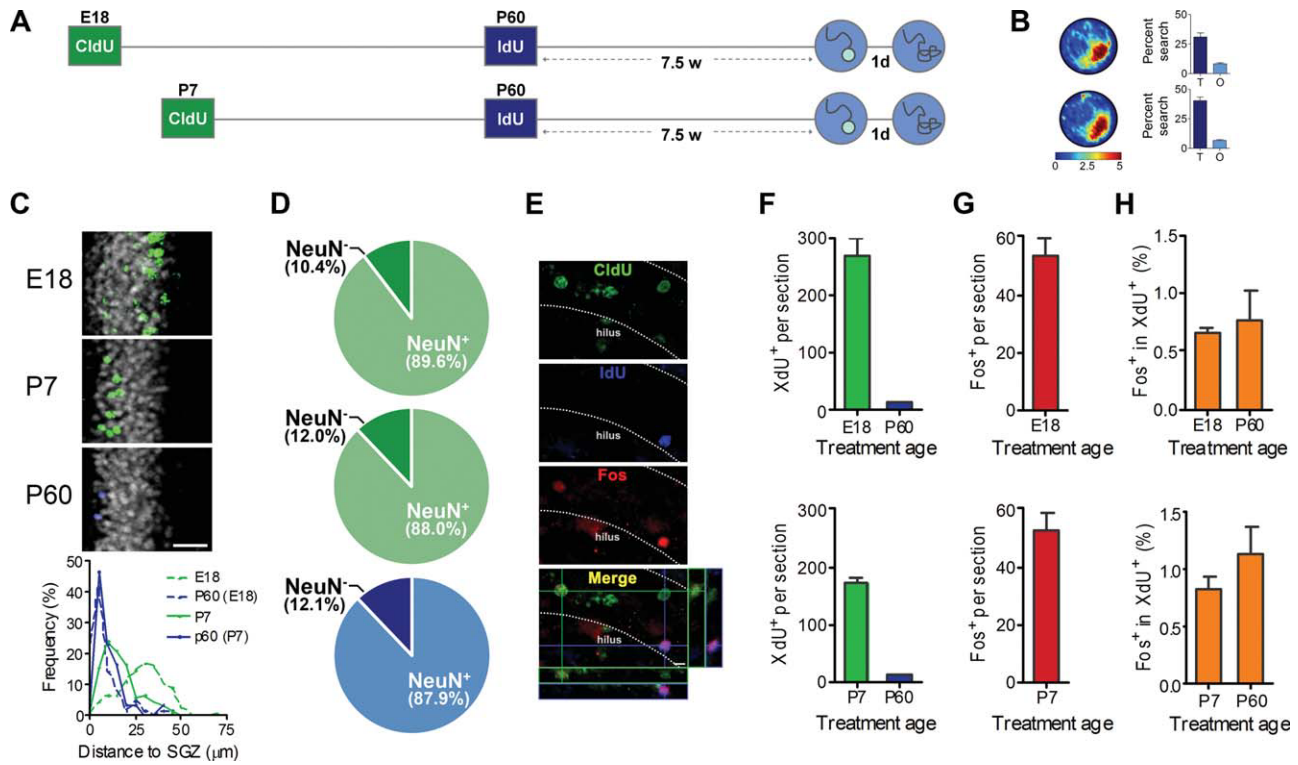

FIGURE 5. Integration of E18, P7, and P60 DGCs (within animal design). A: Experimental design. In Group 1, pregnant mice were treated with CldU at E18, and their progeny with IdU at P60. In Group 2, mouse pups were treated with CldU at P7 and then IdU at P60. Both groups were trained 7.5 weeks after IdU treatment, and spatial memory was assessed one day following the completion of training. B: Both groups searched selectively in the probe test. Left, density plots for grouped data showing where mice concentrated their searches. The color scale represents the number of visits per animal per 5 cm × 5 cm area. Right, both groups spent more time searching the target zone (T) compared with other (O) zones. C: Representative images of DGCs labeled by CldU injection at E18 (top) or P7 (middle) or by IdU injections at P60 (bottom) (DAPI counterstain, scale bar = 20 μm). The lower graph quantifies the relative distributions of embryonically, postnatally, and adult-labeled DGCs. D: Proportion of CldU- or IdU-labeled cells that were NeuN+ following treatment at E18 (top), P7 (middle) or P60 (bottom). E: Representative confocal images of CldU+, IdU+, Fos+ and XdU+/Fos+ (merge) cells in the DG following water maze testing in group 1 (E18/P60) (scale bar = 5 μm). Dotted lines outline the GCL and SGZ. F: XdU- (CldU- or IdU-) labeled cells in the DG for Group 1 (upper) and Group 2 (lower). These were highest in the E18 or P7 group relative to P60, reflecting higher rates of developmental neurogenesis. G: Fos expression in the DG following probe tests was similar for both groups. H: Likelihood of Fos expression in XdU+ cells for both groups following probe tests was similar in corresponding developmentally and adult-generated DGCs, suggesting similar integration rates into DG circuits supporting water maze memory. [Color figure can be viewed in the online issue, which is available at wileyonlinelibrary.com.]

per DG section (indicated as "[cells] per section" throughout the figures) were representative of the entire DG and appropriate for group comparisons. Unless otherwise specified, direct counting of labeled cells, identified by unique point criteria, in the entire DG was performed.

Arc and Fos colocalization was quantified initially using an epifluorescent microscope with a 40× objective. These results were compared to subsets of 50–100 cells per animal analyzed with a 40X/1.3 objective on a confocal microscope. Confocal 1-μm Z-stack optical sections were obtained at 15-μm spaced intervals to prevent duplicate counts of the same cell. In all animals the confocal data matched the epifluorescent results.

The density of Fos+ cells was relatively low (<1.5% of DGCs expressed Fos following behavioral testing) and therefore it was possible to quantify the number of Fos+ cells from images acquired using a 10× or 20× objective.

The total number of NeuN+ cells in the DG was estimated using a method adapted from Barnes and coworkers (Chawla et al., 2005). Two confocal Z-stacks of 1-μm optical sections per DG (one each from the upper and lower blades) were collected from four mice with a 40×/1.3 objective. The total number of NeuN+ cells in each 50-μm stack was counted manually and the total area of the middle plane was measured. From this we calculated the density of NeuN+ cells in the DG. From our analysis of Fos+ cells, we then determined the proportion of NeuN+ cells expressing Fos following behavioral testing and PTZ treatment (see also (Kee et al., 2007b)).

Adult labeled BrdU+ and Fos+/BrdU+ cells were first determined using an epifluorescent microscope with a 40× objective. A subset of Fos+/BrdU+ cells was verified using a 40×/1.3 objective on a confocal microscope.

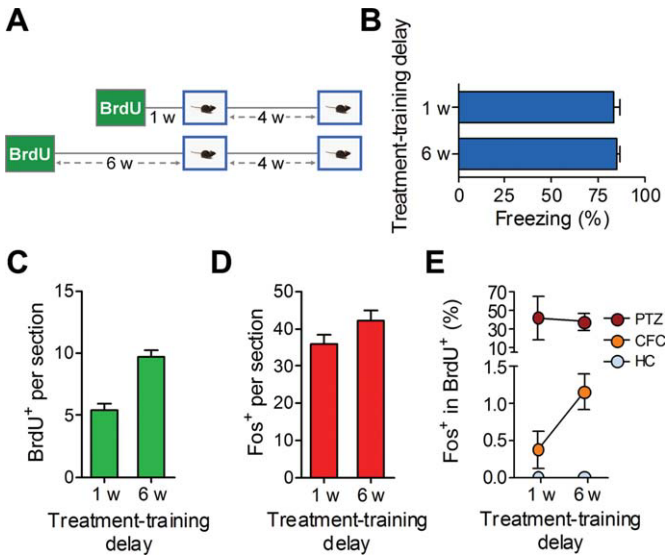

FIGURE 6. Maturation regulates integration of developmentally and adult-generated DGCs into hippocampal circuits supporting contextual fear memory. A: Experimental design. Mice were treated with BrdU and trained in contextual fear conditioning one or six weeks later. Memory was assessed four weeks following training. B: Levels of conditioned freezing were similar in both groups. C: Number of BrdU+ cells was reduced in mice trained one week after BrdU treatment. D: Following memory testing similar numbers of Fos+ cells were identified in the dentate gyrus in both groups. E: Fos expression in BrdU+ cells was significantly higher in mice trained six weeks following BrdU treatment (orange). Fos expression in BrdU+ cells is also shown for the HC (light blue) and PTZ (red) groups. [Color figure can be viewed in the online issue, which is available at wileyonlinelibrary.com.]

The numerous developmentally labeled BrdU+, XdU+, Fos+/BrdU+, and Fos+/XdU+ cells were determined from 4-μm spaced, 1-μm thick, Z-stack optical sections of the entire DG using a 20X objective. Cells were counted by two experimenters (unaware of the treatment conditions). A subset of Fos+/XdU+ cells were confirmed with a 40×/1.3 objective on a confocal microscope. Average counts obtained by the two observers were used in statistical analyses. These Z-stack images were also used to measure the distance of XdU+ cells from the SGZ.

To estimate the proportions of BrdU+ and XdU+ cells that were NeuN+, and to assess the proportions of XdU+ cells that were mono- or colabeled for IdU and/or CldU, randomly chosen DG regions of interest were analyzed using confocal Z-stacks of 1-μm optical sections collected from three mice per group with a 40×/1.3 objective. Approximately 100 BrdU+ or XdU+ cells were counted per animal and assessed for colabeling.

Statistical Analyses

Behavioral and cell counting data were evaluated using parametric ANOVAs or *t*-tests, where appropriate. Post hoc Newman-Keuls tests were used to examine significant main effects or interactions. Statistics were performed using STATISTICA 8.0 software (StatSoft Inc, Tulsa, OK).

RESULTS

Fos Protein in DGCs is Regulated by Memory Recall

The IEG *c-fos* is induced by neural activity, and has been used as an activity marker in a variety of different experimental situations and brain regions (Dragunow and Robertson, 1987; Hunt et al., 1987; Morgan et al., 1987; Saffen et al., 1988; Guzowski et al., 2005). Our current experiments are focused on the DG, and, accordingly, we initially characterized the regulation of Fos in DGCs in a range of conditions. First, recall of a spatial memory induced Fos in ~1% of DGCs, consistent with previous IEG (Chawla et al., 2005) and electrophysiological (Jung and McNaughton, 1993) studies showing that a similarly small proportion of granule cells are activated during spatial exploration. These levels are higher than those in home cage control mice, and much lower than in mice treated with the chemical convulsant, PTZ ($F2,6 = 43.3$, $P < 0.001$) (Fig. 1A). Second, high-frequency electrical stimulation of the major afferent input into the DG leads to an upregulation of Fos in a similarly small subpopulation of DGCs, relative to home cage or nonstimulated controls ($F2,15 = 5.51$, $P < 0.05$) (Fig. 1B). Third, Fos expression is limited to neurons following either behavioral testing or PTZ treatment, as almost all Fos+ cells also expressed the neuronal marker, NeuN (Fig. 1C). Fourth, other IEGs including *Arc* (also known as *Arg3.1*) have been used as activity markers. Following behavioral testing we found similar numbers of Fos+ and Arc+ DGCs, and, these signals were almost completely colocalized. This suggests that Fos and Arc are regulated in a highly similar manner in DGCs (Fig. 1D). Together, these data support the idea that Fos can be used as a neuronal activity marker in the DG, and that Fos is regulated in a similar manner to other IEGs such as Arc.

Integration of Adult-Generated DGCs is Regulated by Maturation

As adult-generated DGCs mature, they exhibit distinct plastic properties compared with their developmentally generated neighbors (Ge et al., 2007). We therefore next evaluated whether such transient changes in plasticity coincide with transient increases in rates at which adult-generated DGCs are integrated into hippocampal memory circuits. To address this question, mice were injected with the proliferation marker BrdU and separate groups were trained in the water maze either 1, 5, 7.5, or 10 weeks later. One day following the completion of training, spatial memory was assessed in a series of probe tests (Fig. 2A). Ninety minutes following testing, mice were perfused and Fos and BrdU expression in DG tissue was quantified using immunohistochemical approaches (Kee et al., 2007b). As

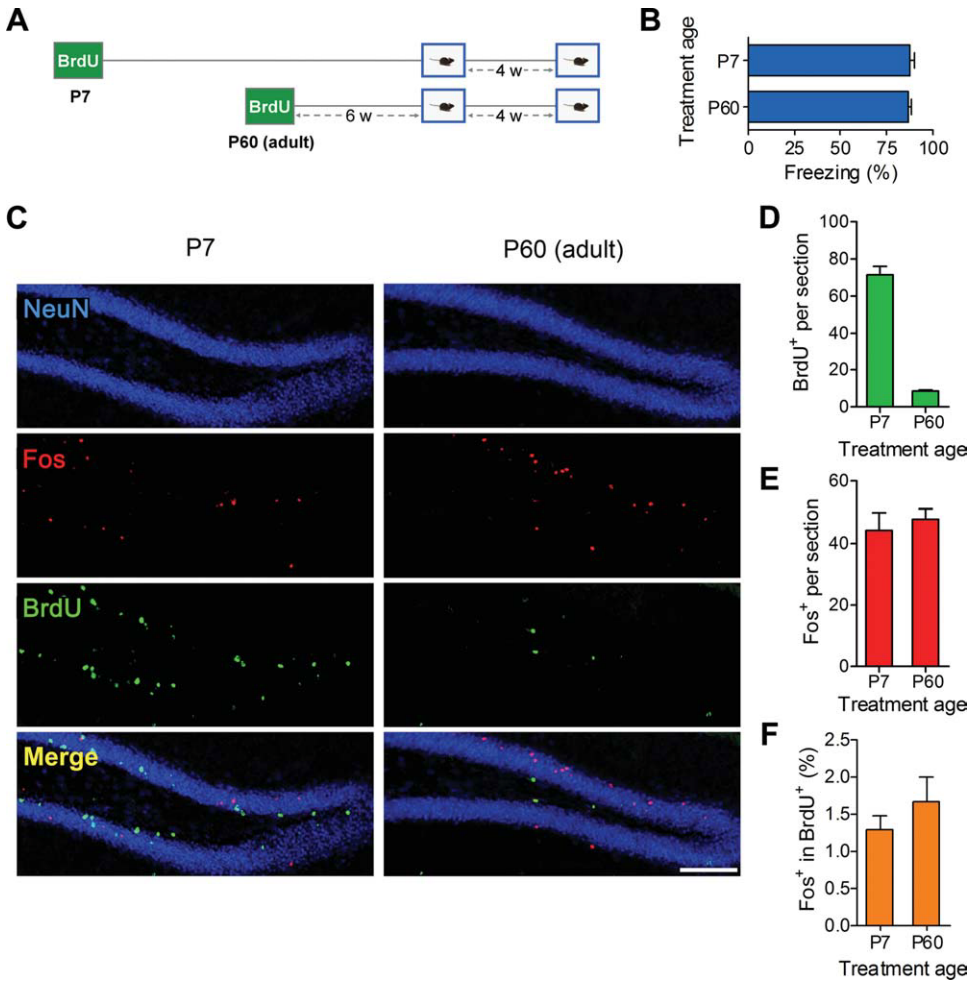

FIGURE 7. Postnatally and adult-generated DGCs integrate at similar rates into hippocampal circuits supporting contextual fear memory. A: Mice were treated with BrdU either at P7 or as adults (P60). At P100 both groups were trained, and contextual fear memory tested one month later. B: Levels of conditioned freezing were similar in both groups. C: Low magnification examples of NeuN, Fos, and BrdU immunofluorescence in the DG following contextual fear testing in the postnatal- (P7) and adult- (P60) treated groups (Scale bar = 100 μm). D: Number of BrdU+ cells was highest in the P7 group, reflecting higher rates of developmental neurogenesis. E: Following contextual fear memory testing, Fos expression in the DG was similar in both groups. F: Fos expression in BrdU+ cells was similar in both groups, suggesting that postnatally and adult-generated cells are integrated at similar rates into DG circuits supporting contextual fear memory. [Color figure can be viewed in the online issue, which is available at wileyonlinelibrary.com.]

Fos expression is regulated by neuronal activity (see Fig. 1), the degree of overlap between BrdU-labeled and Fos-labeled neurons provides an indication of whether adult-generated DGCs have been incorporated into hippocampal memory circuits.

Over the course of training mice required progressively less time to locate the platform, and escape latencies did not differ between groups (Fig. S1A). In the probe test following training, all groups of mice spent significantly more time in the area of the pool that formerly contained the platform (Fig. 2B) (paired *t*-tests; all *P*s < 0.001), indicating that this training produced robust spatial memory. Following the probe test we identified many Fos+ and BrdU+ cells in the DG (Fig. 2C). As expected, the number of BrdU+ cells generally declined as the BrdU-training delay increased ($F_{3,58} = 60.6$, $P < 0.001$) (Fig. 2D), reflecting reduced survival at longer delays. Fos was also expressed in a relatively small proportion (<1.5%) of DGCs, consistent with previous studies (Chawla et al., 2005; Kee et al., 2007a) and the idea that spatial information is sparsely encoded in the DG (Jung and McNaughton, 1993). There were differences in Fos expression between groups (Fig. 2E) ($F_{3,58} = 6.33$, $P < 0.001$) though, with levels in the 1 week group lower than all other groups (*P*s < 0.05). Most notably, overlap between Fos+ and BrdU+ cells depended on the delay between BrdU treatment and training (Fig. 2F). As this delay lengthened, the probability of Fos expression in BrdU+ cells increased ($F_{3,58} = 3.39$, $P < 0.05$), supporting the idea that integration of newborn DGCs into spatial memory networks is regulated by maturation (Kee et al., 2007a). The most marked difference in Fos expression in BrdU+ cells was between the 1 and 5 week groups. At five weeks of age, newborn DGCs ex-

hibit a transient increase in plasticity [i.e., lower induction threshold and increased amplitude LTP (Ge et al., 2007)], and therefore these changes in plasticity might promote integration. Fos expression in BrdU+ cells did not differ in the 5–10 week groups. This suggests that beyond five weeks of age, integration rates stabilized and enhanced plasticity in five-week-old DGCs does not result in a transient increase in rates of functional incorporation.

The ability of newborn cells to express IEGs such as *c-fos* may vary as a function of cell age and/or phenotype (Jessberger and Kempermann, 2003). With regard to cell age, in our experiment the BrdU-labeled cells were ~1-, 5-, 7.5-, and 10-weeks-old at the time of testing. To evaluate whether changes in Fos expression reflect cell-age dependent differences in ability to express Fos, we additionally examined Fos expression in a home cage condition or following treatment with a chemical convulsant, PTZ, in BrdU-treated matched controls. In the home cage condition, Fos expression was uniformly low in all groups (Fig. 2F). In contrast, PTZ treatment induced robust Fos expression in BrdU+ cells, but these levels were appreciably higher in the 5–10 week groups compared with the one-week group ($F3,7 = 13.9$, $P < 0.005$) (Fig. 2F). Therefore, these nonphysiological conditions, where activity levels are driven toward ceiling, reveal cell age-dependent differences in Fos regulation (Jessberger and Kempermann, 2003). Accordingly, they suggest that the low levels of Fos expression in BrdU+ cells in the mice trained one week following BrdU treatment likely reflect an inability of week-old DGCs to express Fos, rather than an inability of these newborn cells to integrate.

To address this confound, an additional group of mice were trained one week after BrdU treatment, and tested four weeks, rather than one day, later (Fig. 2A). This ensures that BrdU-labeled cells are the same age at the time of testing as those in the five-week group. In the probe test, mice searched selectively (paired *t*-test, $P < 0.001$; Fig. 2B). Following the probe test numerous Fos+ and BrdU+ cells were identified in the DG (Figs. 2D–E), and these levels were equivalent to those in the five-week group (Ps >0.05). Most importantly, there was little overlap between these two populations of cells (Fig. 2F): The likelihood of Fos expression in BrdU-labeled cells was significantly lower than in the five-week group ($P < 0.05$) and no different to those in the one week ($P = 0.39$) or home cage ($P = 0.61$) groups. Therefore, controlling for cell-age confounds, this experiment indicates that week-old adult-generated DGCs are insufficiently mature to be incorporated into spatial networks in the DG, consistent with our previous report (Kee et al., 2007a). The direct comparison of these two groups allows us to rule out three alternative interpretations of the data. First, the fixed delay between BrdU treatment and testing ensures that all labeled cells are the same age at the time of testing. Therefore, any group differences in Fos expression in BrdU+ cells are unlikely to be due to differences in maturation. Second, differential levels of Fos expression between groups indicate that five-week-old adult-generated neurons do not simply have a lower threshold for activation during memory retrieval. Third, mice in each group underwent exactly the same experience immediately prior to sacrifice, and therefore group differences in numbers of Fos+/BrdU+ cells are specifically related to spatial memory processing and not related to nonspecific aspects of the testing procedure (e.g., handling, activity, mild stress, or arousal).

After behavioral testing, induction of Fos is almost exclusively neuronal in the granule cell layer (GCL) of the DG [Figs. 1A,B; see also (Kee et al., 2007a,b)]. Therefore, a second potential confound is that differences in Fos expression in BrdU+ cells reflect group differences in the proportion of BrdU-labeled cells that differentiated into neurons. To address this issue, we counterstained for the neuronal marker, NeuN, in the groups of mice trained in the water maze 1, 5, and 10 weeks following BrdU treatment. Consistent with previous studies (Brandt et al., 2003), we found that BrdU+ cells were equivalently likely to be NeuN+ across groups (Fig. 2G) ($F2,6 = 0.13$, $P = 0.89$), indicating that group differences in BrdU+ cell phenotype cannot account for differences in Fos expression in BrdU+ cells.

Finally, it is important to note that in the 5–10 week groups, rates of Fos expression in BrdU+ cells were greater than those in NeuN+ cells (Fig. 2F), as in our previous study (Kee et al., 2007a) (see also Fig. S2). While this may suggest that adult-generated DGCs are recruited preferentially, Fos expression in NeuN+ cells provides only an indirect estimate of integration rates for developmentally generated DGCs. As NeuN is expressed in both immature [as young as three-day-old: (Brandt et al., 2003)] as well mature neurons, these analyses might underestimate integration rates of developmentally generated DGCs. To address this we will label developmentally generated DGCs directly in the following experiments.

Integration of Equivalently Aged E18, P7, and P60 DGCs

In the developing brain, two major waves of neurogenesis lead to the formation of the DG (Schlessinger et al., 1975; Altman and Bayer, 1990; Piatti et al., 2006). First, late in embryonic development (E15-P1), neural progenitor cells in the secondary dentate matrix generate DGCs that form the outer shell of the upper, and subsequently, lower blade of the DG. A second dentate migration after birth (>P1) leads to the formation of the tertiary dentate matrix, and neural progenitor cells from here migrate radially and generate DGCs that populate the inner part of the GCL. These neural progenitor cells subsequently accumulate in the SGZ and continue to generate DGCs throughout adulthood (albeit at exponentially declining levels). In the above experiment we found that adult-generated DGCs are integrated into spatial memory circuits in a maturation-dependent manner, and once new neurons are five weeks or more in age integration rates remained relatively stable. One key question is whether these stable rates of integration of mature adult-generated DGCs differ from those of developmentally generated DGCs.

To address this question, three groups of mice were treated with BrdU at E18, P7, or as adults (P60). To ensure that BrdU-labeled cells were equivalently aged at the time of training and testing, all groups were trained 7.5 weeks after BrdU treatment (Figs. 3A, S1B). In the probe test conducted one day following the completion of training, all groups of mice searched selectively in the region of the pool that formerly contained the platform (Fig. 3B) (paired *t*-tests, $P < 0.01$). Following the probe test, immunohistochemical processing revealed many Fos+ and BrdU+ cells in the DG. Decreasing numbers of BrdU+ cells were found following treatment at E18, P7, and P60, respectively (Fig. 3C) ($F2,27 = 181.0$, $P < 0.001$), reflecting age-dependent decline in rates of proliferation. In contrast, the numbers of Fos+ cells were similar across groups (Fig. 3D) ($F2,27 = 0.49$, $P = 0.61$). Most importantly, we found that the likelihood of Fos expression in BrdU+ cells did not differ between groups following the probe test (Fig. 3E) ($F2,27 = 0.20$, $P = 0.82$), indicating that integration rates of equivalently aged DGCs are the same, regardless of whether they were born during development (E18, P7) or in adulthood (P60). We found the same pattern of results in an additional experiment where mice were treated with PTZ to strongly activate DGCs. Similar to the water maze experiment, we found that Fos expression in BrdU+ cells did not differ between E18, P7, and P60 groups (Fig. 3F) ($F2,6 = 3.17$, $P = 0.12$). Together, these experiments suggest that equivalently aged DGCs respond similarly to both physiological and nonphysiological stimulation, regardless of whether they were born during development (E18, P7) or in adulthood (P60).

Recruitment of Adult- vs. Developmentally Generated Granule Cells (Within Animal Comparison)

The previous experiment indicated that equivalently aged DGCs are integrated into circuits supporting spatial memory at similar rates, regardless of whether they were born during development (E18, P7) or in adulthood (P60). A remaining possibility is that, in the adult mouse, more recently adult-generated DGCs out-compete relatively older DGCs that were born during embryonic or early postnatal development. To address this question we next labeled embryonically or postnatally generated DGCs and directly compared their integration rates with adult-generated DGCs in the same animal. To achieve this within-animal comparison mice were treated with two equimolar, chemically related thymidine analogs, CldU and IdU (Tronel et al., 2010; Burns and Kuan, 2005; Vega and Peterson, 2005; Dupret et al., 2007; Thomas et al., 2007). CldU and IdU are recognized by different antibodies and so separate cohorts of cells may be labeled in the same mice. We first verified that our staining procedures detected CldU and IdU specifically within mice exposed to both compounds (Leuner et al., 2009). To do this, mice were first injected with CldU at P7 and then IdU at P60 (or vice versa). Tissue from all animals was subjected to identical staining (i.e., incubated with primary and secondary antibodies for both compounds), and many DGCs were identified (Fig. 4A). Importantly, virtually no DGCs were labeled for both IdU and CldU (Fig. 4B), indicating that staining was specific for each compound. Furthermore, there were similar numbers of CldU- and IdU-labeled DGCs at both time points and in both groups (Fig. 4C) ($F1,5 = 0.35$, $P = 0.58$), indicating that these compounds label equivalent numbers of DGCs. Similar experiments performed in adult mice in which animals were injected with either one of the compounds at P60, confirmed the near absence of cross-detection (Fig. S3). Importantly, when adult mice received CldU and IdU simultaneously, virtually all cells were colabeled as expected (Fig. 4D). Together these results indicate that, using our methodology, CldU and IdU can be used in the same animal to specifically label separate cohorts of DGCs with equivalent sensitivity.

To label embryonically generated and adult-generated DGCs in the same mice, pregnant mice were injected with CldU at E18 and then their progeny were subsequently treated with IdU once they reached adulthood (P60). To label postnatally generated and adult-generated DGCs in the same mice, mouse pups were treated with CldU at P7, and then with IdU after they reached adulthood (P60). Both groups of mice were then trained in the water maze 7.5 weeks following IdU treatment (Fig. S1C) and spatial memory was assessed one day following the completion of training (Fig. 5A). In the probe test, both groups of mice concentrated their search in the region of the pool that formerly contained the platform (Fig. 5B) (paired *t*-tests, $P < 0.01$). Following the probe test, many CldU+, IdU+, and Fos+ cells were identified in the DG. Importantly, the distribution and number (but not phenotype) of CldU+ and IdU+ cells depended on the timing of the treatment. First, while embryonically labeled DGCs were distributed throughout the GCL, postnatally generated DGCs were predominantly located in the inner two thirds of the GCL and adult-generated DGCs were largely restricted to the innermost third of the GCL or subgranular zone (Fig. 5C). These distinct distributions reflect the sequential waves of neurogenesis that lead to the formation of the DG during development (Piatti et al., 2006). Second, as treatment age increased the number of labeled cells declined (Figs. 5E,F) (paired *t*-test [E18/P60]: $t11 = 9.16$, $P < 0.001$; paired *t*-test [P7/P60]: $t13 = 17.9$, $P < 0.001$), reflecting an age-dependent decline in proliferation. Third, embryonically generated, postnatally generated, and adult-generated cells were equally likely to differentiate into neurons (Fig. 5D) ($F2,6 = 0.79$, $P = 0.50$). Following the probe test, similar numbers of Fos+ cells were identified in the DG in both groups (Figs. 5E,G) ($t24 = 0.04$, $P = 0.97$). Most strikingly, developmentally generated and adult-generated DGCs appeared to be recruited at equivalent rates into DG circuits supporting spatial memory: The likelihood of Fos expression in embryonically generated or postnatally generated cells did not differ to that in adult-generated cells (Figs. 5E,H) (paired *t*-test [E18/P60]: $t11 = 0.39$, $P = 0.70$; paired *t*-test [P7/P60]: $t13 = 1.03$, $P = 0.32$). Counter to the idea that adult-generated neurons are recruited preferentially into DG memory circuits, these data suggest that they are recruited at

equivalent rates to those of existing (or developmentally generated) DGCs.

Contextual Fear Conditioning

The above experiments suggest that developmentally generated and adult-generated DGCs are recruited at similar rates into hippocampal circuits supporting water maze memory. Since the hippocampus is engaged in a wide range of learning situations, we finally wanted to determine whether this pattern of results would generalize to another form of hippocampus-dependent learning such as contextual fear conditioning (Kim and Fanselow, 1992). In our first experiment we evaluated whether the integration of adult-generated DGCs into hippocampal networks supporting contextual fear memory depends on cell age, as is the case in the water maze (Kee et al., 2007a). In this experiment mice were treated with BrdU, and then trained in contextual fear conditioning either one week or six weeks later (Fig. 6A). During the retention test four weeks later, all mice exhibited similar levels of conditioned freezing ($t26 = 0.45$, $P = 0.66$) (Fig. 6B). Furthermore, we identified similar numbers of Fos+ cells ($t26 = 1.38$, $P = 0.18$) (Fig. 6D). Notably, numbers of BrdU+ cells were decreased in mice trained one week following BrdU treatment ($t26 = 5.17$, $P < 0.001$) (Fig. 6C). This might suggest that mild stress associated with training episode was sufficient to reduce survival of relatively immature (i.e., one-week-old but not six-week-old) adult-born cells, an observation that is consistent with the idea that stress regulates the survival of newborn cells (Gould et al., 1991). Most importantly, after normalizing for the number of BrdU+ cells, we found that the likelihood of Fos expression in BrdU+ cells was higher in the group of mice treated with BrdU six weeks before training ($t26 = 2.12$, $P < 0.05$) (Fig. 6E). These differences in overlap were not due to either cell age-dependent differences in ability to express Fos between groups, since PTZ-induced Fos expression was similar in age-matched controls (Fig. 6E) ($t3 = 0.18$, $P = 0.87$), or the age of the memory at the time of testing (Figs. S4A-E). Furthermore, this maturation-dependent pattern of integration was limited to the DG and did not extend to the olfactory bulb (Figs. S4F-H), another neurogenic region in the adult brain that would not be expected to play a major role in contextual fear conditioning [for similar results in water maze see: (Kee et al., 2007a)]. Consistent with the water maze, these data support the idea that adult-generated DGCs are integrated into hippocampal networks supporting contextual fear conditioning memories (Saxe et al., 2006; Winocur et al., 2006; Warner-Schmidt et al., 2008; Deng et al., 2009a,b; Hernandez-Rabaza et al., 2009; Ko et al., 2009), and establish that integration depends on their maturational state.

Using a between subjects design, we next tested whether developmentally generated and adult-generated DGCs are recruited at similar rates into hippocampal networks supporting contextual fear memory. Mice were treated with BrdU either at P7 or during adulthood (P60) (Fig. 7A). Both groups were then trained at P100 and tested one month later. In this test, conditioned freezing levels were similar in both groups of mice ($t31 = 0.37$, $P = 0.71$) (Fig. 7B), indicating that training produced robust contextual fear memory. We identified significantly more BrdU+ cells in mice treated with BrdU at P7 compared to adulthood ($t31 = 27.6$, $P < 0.001$) (Figs. 7C,D), reflecting higher rates of neurogenesis during the early postnatal period. Contextual fear conditioning testing induced Fos in the DGCs, and expression levels were similar between groups ($t31 = 0.44$, $P = 0.67$) (Figs. 7C,E). Most notably, the likelihood of Fos expression in BrdU+ cells did not differ between groups ($t31 = 0.55$, $P = 0.58$) (Fig. 7F), suggesting that DGCs generated during the postnatal period and adulthood are equally likely to become integrated into DG circuits supporting contextual fear memory. We further replicated these findings in a separate experiment using a within subject design (Fig. S5). Therefore, using a task with quite different stimulus properties and performance demands (but nonetheless dependent upon the hippocampus) these data provide convergent evidence that developmentally generated and adult generated DGCs are integrated at similar rates into hippocampal memory networks.

DISCUSSION

The persistence of neurogenesis in the hippocampus beyond development means that the adult DG is composed of a heterogeneous pool of developmentally generated and adult-generated granule cells. While both developmentally generated and adult-generated DGCs are believed to contribute to hippocampal memory processing, whether they represent functionally equivalent or distinct pools of neurons is not known. Here we used immunohistochemical procedures to study the activation of developmentally generated and adult-generated DGCs following memory recall. Four main lines of evidence suggest that developmentally generated and adult-generated DGCs were equally likely to contribute to hippocampal memory formation. First, using a water maze task, we found that after adult-generated DGCs reached five weeks of age, integration rates stabilized. There was no evidence for a transient peak in integration rates that might correspond with known changes in plasticity in maturing, adult-generated DGCs (Ge et al., 2007). Second, 7.5-week-old DGCs are integrated into circuits supporting water maze memory at similar rates, regardless of whether they were born during embryonic or postnatal development or during adulthood. Third, while the adult DG is composed of neurons generated during development and during adulthood, we found corresponding integration rates for embryonically generated, postnatally generated, and adult-generated DGCs in our within-animal comparison. Finally, we found similar rates of integration for developmentally generated and adult-generated DGCs in another hippocampus-dependent task-contextual fear conditioning. Collectively, these results provide convergent evidence that developmentally generated and adult-generated DGCs are integrated at similar rates into hippocampal memory networks, and suggest a functional equivalence between DGCs generated at different developmental stages.

In these studies we quantified the expression of the IEG, *c-fos*, in order to identify newborn DGCs exhibiting memory-related activation. Fos expression is regulated by neural activity and therefore has been used to map neural activation following, for example, seizures (Dragunow and Robertson 1987; Morgan et al., 1987; Saffen et al., 1988), induction of NMDA-dependent LTP (Cole et al., 1989; Dragunow et al., 1989; Worley et al., 1993), noxious stimulation (Hunt et al., 1987) as well as learning and/or memory recall (Guzowski et al., 2005). Here we showed that both memory recall and stimulation of DG afferents leads to the specific upregulation of Fos in DGCs, and that another IEG product, Arc, is similarly upregulated in the same subpopulation. While several studies have established that newborn DGCs express IEGs in various experimental situations (Jessberger and Kempermann 2003; Ramirez-Amaya et al., 2006; Kee et al., 2007a; Tashiro et al., 2007; Farioli-Vecchioli et al., 2008; Takahashi et al., 2009), the major challenge in memory studies is to develop experimental designs that can differentiate between gene expression associated with memory processing from that associated with nonspecific aspects of the testing procedure. Our experiments typically included three sequential components-treatment of mice with thymidine analogs (BrdU, IdU, CldU), training and memory testing-the relative timing of which was manipulated across experiments. The critical feature common to all experiments is that all groups underwent exactly the same experience prior to sacrifice. That is, all mice were removed from their home cage, transported to the testing room, and expressed a spatial or fear memory. Therefore, this ensures that observed between-group differences in Fos expression in thymidine analog-labeled cells (see Figs. 2F and 6E) cannot be attributed to these general features of the testing experience. Accordingly, here we confirmed that integration of newborn DGCs into hippocampal circuits supporting water maze memory is regulated by cell age, with newborn DGCs not maximally contributing until they are five weeks or older (Kee et al., 2007a). This delayed time course for functional integration follows the establishment and gradual maturation of excitatory connections of newborn DGCs (Piatti et al., 2006; Zhao et al. 2008).

In this study, spatial memory recall induced Fos expression in only a small proportion of mature adult-generated DGCs, consistent with the idea that spatial information is sparsely encoded in the DG (Jung and McNaughton 1993; Chawla et al., 2005). Subsequent experiments established that these levels were not different to those in developmentally generated DGCs. This was observed across a range of experimental conditions: When the age of developmentally generated and adult-generated DGCs was matched (Experiment 3), in a within-mouse comparison (where animal age was fixed, but cell age varied; Experiment 5) and using a contextual fear conditioning paradigm (Experiment 7). Not in one experiment was the null hypothesis-that developmentally generated and adult-generated DGCs are integrated into hippocampal memory circuits at equivalent rates-rejected, and therefore, collectively, these experiments provide no support that the alternative-that developmentally generated and adult-generated DGCs are integrated into hippocampal memory circuits at different rates-is true. The lack of evidence for preferential recruitment of adult-generated DGCs is consistent with previous studies establishing that, once they reach maturity, adult-generated DGCs exhibit similar neuronal phenotypes as developmentally generated DGCs (Laplagne et al., 2006; Zhao et al., 2006; Laplagne et al., 2007). For example, developmentally generated and adult-generated DGCs eventually establish equivalent afferent and efferent connectivity, exhibit similar morphology and electrophysiological properties (excitability and short- and long-term plasticity) (Laplagne et al., 2006; Zhao et al., 2006; Ge et al., 2007; Laplagne et al., 2007; Toni et al., 2007; Toni et al., 2008). Therefore, in addition to this phenotypic convergence at the anatomical, morphological, and electrophysiological levels, the current series of experiments provide evidence for similar convergence at the behavioral level. They suggest that developmentally generated and adult-generated DGCs are interchangeable, as long as they are sufficiently mature. Such phenotypic convergence is typical in other organ systems, including skin, blood, muscle, liver, etc and would be advantageous for potential cell replacement therapies: That is, that stimulation of adult neurogenesis would lead to the repopulation of the DG with functionally equivalent cell-types (or replacing like with like).

Our experiments do not support the idea that adult-generated DGCs are recruited preferentially relative to developmentally generated cells, and stands in contrast to the conclusions of some previous studies (Ramirez-Amaya et al., 2006; Tashiro et al., 2007) including our own (Kee et al., 2007a). In these previous studies, BrdU was injected into adult mice to label adult-generated DGCs (as in the current experiments). However, unlike the current experiments, developmentally generated DGCs were not labeled directly. Rather, IEG expression was examined in BrdU-labeled (adult-generated) cells vs. NeuN-labeled cells in the same animals. NeuN may be expressed in cells as young as three days old (Brandt et al., 2003). Therefore, as the DG is composed of a heterogeneous pool of immature and mature NeuN+ cells (and adult-generated DGCs <2 weeks old do not express Fos) (Jessberger and Kempermann 2003), these analyses likely underestimate recruitment rates for developmentally generated cells. In the current experiments, we confirmed that the likelihood of Fos expression in BrdU+ cells was significantly higher than in NeuN+ cells (Figs. 2F and S2).

Our finding that developmentally-generated and adult-generated DGCs are integrated at similar rates is not incompatible with the idea that adult neurogenesis plays a critical role in hippocampal memory. Indeed, suppression of adult neurogenesis disrupts multiple forms of hippocampal-dependent learning, including the water maze and contextual fear conditioning (Deng et al., 2009a,b; Shors, 2008). This suggests that (at least in some conditions) normal levels of neurogenesis are essential for hippocampal memory function. Instead, it might be more appropriate to consider that the critical contribution of adult neurogenesis to hippocampal memory function is at the network, rather than cellular, level. For example, the addition of

new DGCs into hippocampal circuitry may degrade existing memories (Meltzer et al., 2005), and such degradation may promote the transformation of memories from hippocampal-dependent to hippocampal-independent forms in the cortex (Feng et al., 2001; Kitamura et al., 2009).

Comparison of integration rates of developmentally- and adult-generated DGCs makes it possible to estimate the overall contribution of adult-generated DGCs to hippocampal memory networks. Given our finding that developmentally-generated and adult-generated cells were recruited at similar rates, the contribution of adult-generated DGCs to hippocampal memory processing should be directly proportional to their number. In young adult mice, adult-generated cells constitute as much as 15% of the DG (Ninkovic et al., 2007; Imayoshi et al., 2008), and so 15% of DGCs contributing to memory-related activity in the DG would be predicted to be have been generated during adulthood. As levels of neurogenesis are modulated across the lifespan (Kuhn et al., 1996) and by environmental factors, such as enrichment and/or exercise (Kempermann et al., 1997; van Praag et al., 1999), this model would then predict that under conditions where levels of adult neurogenesis decline [e.g., with age (Kuhn et al., 1996)], the contribution of adult-born neurons to hippocampal memory function declines proportionally.

Finally, in order to label separate cohorts of new neurons within the same animal, we used the thymidine analogs CldU and IdU along with immunohistochemical procedures designed to recognize one or the other exclusively (Tronel et al., 2010; Burns and Kuan, 2005; Vega and Peterson, 2005; Dupret et al., 2007; Thomas et al., 2007). Although techniques vary among these reports and can lead to cross-detection (Leuner et al., 2009), we established that our injection and immunohistochemistry methods did not result in nonspecific labeling of one compound by both primary antibodies. Consistent with (Leuner et al., 2009), we also found no difference in the sensitivity of cell-labeling between the two compounds (although sensitivity levels may be below that of BrdU).

Acknowledgments

The authors thank Sheena Josselyn for comments on this manuscript, and Nohjin Kee and Na Hyea Kang for technical assistance.

REFERENCES

Aimone JB, Wiles J, Gage FH. 2006. Potential role for adult neurogenesis in the encoding of time in new memories. Nat Neurosci 9:723–727.

Aimone JB, Wiles J, Gage FH. 2009. Computational influence of adult neurogenesis on memory encoding. Neuron 61:187–202.

Altman J, Bayer SA. 1990. Migration and distribution of two populations of hippocampal granule cell precursors during the perinatal and postnatal periods. J Comp Neurol 301:365–381.

Bick-Sander A, Steiner B, Wolf SA, Babu H, Kempermann G. 2006. Running in pregnancy transiently increases postnatal hippocampal neurogenesis in the offspring. Proc Natl Acad Sci USA 103:3852–3857.

Brandt MD, Jessberger S, Steiner B, Kronenberg G, Reuter K, et al. 2003. Transient calretinin expression defines early postmitotic step of neuronal differentiation in adult hippocampal neurogenesis of mice. Mol Cell Neurosci 24:603–613.

Burns KA, Kuan CY. 2005. Low doses of bromo- and iododeoxyuridine produce near-saturation labeling of adult proliferative populations in the dentate gyrus. Eur J Neurosci 21:803–807.

Chawla MK, Guzowski JF, Ramirez-Amaya V, Lipa P, Hoffman KL, et al. 2005. Sparse, environmentally selective expression of Arc RNA in the upper blade of the rodent fascia dentata by brief spatial experience. Hippocampus 15:579–586.

Cole AJ, Saffen DW, Baraban JM, Worley PF. 1989. Rapid increase of an immediate early gene messenger RNA in hippocampal neurons by synaptic NMDA receptor activation. Nature 340:474–476.

Deng W, Aimone JB, Gage FH. 2009a. New neurons and new memories: How does adult hippocampal neurogenesis affect learning and memory? Nat Rev Neurosci 11:339–350.

Deng W, Saxe MD, Gallina IS, Gage FH. 2009b. Adult-born hippocampal dentate granule cells undergoing maturation modulate learning and memory in the brain. J Neurosci 29:13532–13542.

Dragunow M, Robertson HA. 1987. Kindling stimulation induces c-fos protein(s) in granule cells of the rat dentate gyrus. Nature 329:441–442.

Dragunow M, Abraham WC, Goulding M, Mason SE, Robertson HA, et al. 1989. Long-term potentiation and the induction of c-fos mRNA and proteins in the dentate gyrus of unanesthetized rats. Neurosci Lett 101:274–280.

Dupret D, Fabre A, Dobrossy MD, Panatier A, Rodriguez JJ, et al. 2007. Spatial learning depends on both the addition and removal of new hippocampal neurons. PLoS Biol 5:e214.

Farioli-Vecchioli S, Saraulli D, Costanzi M, Pacioni S, Cina I, et al. 2008. The timing of differentiation of adult hippocampal neurons is crucial for spatial memory. PLoS Biol 6:e246.

Feng R, Rampon C, Tang YP, Shrom D, Jin J, et al. 2001. Deficient neurogenesis in forebrain-specific presenilin-1 knockout mice is associated with reduced clearance of hippocampal memory traces. Neuron 32:911–926.

Ge S, Yang CH, Hsu KS, Ming GL, Song H. 2007. A critical period for enhanced synaptic plasticity in newly generated neurons of the adult brain. Neuron 54:559–566.

Gould E, Woolley CS, Cameron HA, Daniels DC, McEwen BS. 1991. Adrenal steroids regulate postnatal development of the rat dentate gyrus. II. Effects of glucocorticoids and mineralocorticoids on cell birth. J Comp Neurol 313:486–493.

Guzowski JF, Timlin JA, Roysam B, McNaughton BL, Worley PF, et al. 2005. Mapping behaviorally relevant neural circuits with immediate-early gene expression. Curr Opin Neurobiol 15:599–606.

Hernandez-Rabaza V, Llorens-Martin M, Velazquez-Sanchez C, Ferragud A, Arcusa A, et al. 2009. Inhibition of adult hippocampal neurogenesis disrupts contextual learning but spares spatial working memory, long-term conditional rule retention and spatial reversal. Neuroscience 159:59–68.

Hunt SP, Pini A, Evan G. 1987. Induction of c-fos-like protein in spinal cord neurons following sensory stimulation. Nature 328:632–634.

Imayoshi I, Sakamoto M, Ohtsuka T, Takao K, Miyakawa T, et al. 2008. Roles of continuous neurogenesis in the structural and functional integrity of the adult forebrain. Nat Neurosci 11:1153–1161.

Jessberger S, Kempermann G. 2003. Adult-born hippocampal neurons mature into activity-dependent responsiveness. Eur J Neurosci 18: 2707–2712.

Jung MW, McNaughton BL. 1993. Spatial selectivity of unit activity in the hippocampal granular layer. Hippocampus 3:165–182.

Kee N, Teixeira CM, Wang AH, Frankland PW. 2007a. Preferential incorporation of adult-generated granule cells into spatial memory networks in the dentate gyrus. Nat Neurosci 10:355–362.

Kee N, Teixeira CM, Wang AH, Frankland PW. 2007b. Imaging activation of adult-generated granule cells in spatial memory. Nat Protoc 2:3033–3044.

Kempermann G, Kuhn HG, Gage FH. 1997. More hippocampal neurons in adult mice living in an enriched environment. Nature 386:493–495.

Kim JJ, Fanselow MS. 1992. Modality-specific retrograde amnesia of fear. Science 256:675–677.

Kitamura T, Saitoh Y, Takashima N, Murayama A, Niibori Y, et al. 2009. Adult neurogenesis modulates the hippocampus-dependent period of associative fear memory. Cell 139:814–827.

Ko HG, Jang DJ, Son J, Kwak C, Choi JH, et al. 2009. Effect of ablated hippocampal neurogenesis on the formation and extinction of contextual fear memory. Mol Brain 2:1.

Kolb B, Pedersen B, Ballermann M, Gibb R, Whishaw IQ. 1999. Embryonic and postnatal injections of bromodeoxyuridine produce age-dependent morphological and behavioral abnormalities. J Neurosci 19:2337–2346.

Kuhn HG, Dickinson-Anson H, Gage FH. 1996. Neurogenesis in the dentate gyrus of the adult rat: Age-related decrease of neuronal progenitor proliferation. J Neurosci 16:2027–2033.

Laplagne DA, Kamienkowski JE, Esposito MS, Piatti VC, Zhao C, et al. 2007. Similar GABAergic inputs in dentate granule cells born during embryonic and adult neurogenesis. Eur J Neurosci 25: 2973–2981.

Laplagne DA, Esposito MS, Piatti VC, Morgenstern NA, Zhao C, et al. 2006. Functional convergence of neurons generated in the developing and adult hippocampus. PLoS Biol 4:e409.

Leuner B, Glasper ER, Gould E. 2009. Thymidine analog methods for studies of adult neurogenesis are not equally sensitive. J Comp Neurol 517:123–133.

Meltzer LA, Yabaluri R, Deisseroth K. 2005. A role for circuit homeostasis in adult neurogenesis. Trends Neurosci 28:653–660.

Ming GL, Song H. 2005. Adult neurogenesis in the mammalian central nervous system. Annu Rev Neurosci 28:223–250.

Morgan JI, Cohen DR, Hempstead JL, Curran T. 1987. Mapping patterns of c-fos expression in the central nervous system after seizure. Science 237:192–197.

Ninkovic J, Mori T, Gotz M. 2007. Distinct modes of neuron addition in adult mouse neurogenesis. J Neurosci 27:10906–10911.

Paxinos G, Franklin KBJ. 2000. The Mouse Brain in Stereotaxic Coordinates. San Diego, CA: Academic Press.216 p.

Piatti VC, Esposito MS, Schinder AF. 2006. The timing of neuronal development in adult hippocampal neurogenesis. Neuroscientist 12:463–468.

Ramirez-Amaya V, Marrone DF, Gage FH, Worley PF, Barnes CA. 2006. Integration of new neurons into functional neural networks. J Neurosci 26:12237–12241.

Saffen DW, Cole AJ, Worley PF, Christy BA, Ryder K et al. 1988. Convulsant-induced increase in transcription factor messenger RNAs in rat brain. Proc Natl Acad Sci USA 85:7795–7799.

Saxe MD, Battaglia F, Wang JW, Malleret G, David DJ et al. 2006. Ablation of hippocampal neurogenesis impairs contextual fear conditioning and synaptic plasticity in the dentate gyrus. Proc Natl Acad Sci USA 103:17501–17506.

Schlessinger AR, Cowan WM, Gottlieb DI. 1975. An autoradiographic study of the time of origin and the pattern of granule cell migration in the dentate gyrus of the rat. J Comp Neurol 159: 149–175.

Schmidt-Hieber C, Jonas P, Bischofberger J. 2004. Enhanced synaptic plasticity in newly generated granule cells of the adult hippocampus. Nature 429:184–187.

Shors TJ. 2008. From stem cells to grandmother cells: How neurogenesis relates to learning and memory. Cell Stem Cell 3:253–258.

Takahashi T, Zhu Y, Hata T, Shimizu-Okabe C, Suzuki K, et al. 2009. Intracranial self-stimulation enhances neurogenesis in hippocampus of adult mice and rats. Neuroscience 158:402–411.

Tashiro A, Makino H, Gage FH. 2007. Experience-specific functional modification of the dentate gyrus through adult neurogenesis: A critical period during an immature stage. J Neurosci 27:3252–3259.

Teixeira CM, Pomedli SR, Maei HR, Kee N, Frankland PW. 2006. Involvement of the anterior cingulate cortex in the expression of remote spatial memory. J Neurosci 26:7555–7564.

Thomas RM, Hotsenpiller G, Peterson DA. 2007. Acute psychosocial stress reduces cell survival in adult hippocampal neurogenesis without altering proliferation. J Neurosci 27:2734–2743.

Toni N, Teng EM, Bushong EA, Aimone JB, Zhao C, et al. 2007. Synapse formation on neurons born in the adult hippocampus. Nat Neurosci 10:727–734.

Toni N, Laplagne DA, Zhao C, Lombardi G, Ribak CE, et al. 2008. Neurons born in the adult dentate gyrus form functional synapses with target cells. Nat Neurosci 11:901–907.

Tronel S, Fabre A, Charrier V, Oliet SH, Gage FH, et al. 2010. Spatial learning sculpts the dendritic arbor of adult-born hippocampal neurons. Proc Natl Acad Sci USA 107:7963–7968.

van Praag H, Kempermann G, Gage FH. 1999. Running increases cell proliferation and neurogenesis in the adult mouse dentate gyrus. Nat Neurosci 2:266–270.

Vega CJ, Peterson DA. 2005. Stem cell proliferative history in tissue revealed by temporal halogenated thymidine analog discrimination. Nat Methods 2:167–169.

Wang SH, Teixeira CM, Wheeler AL, Frankland PW. 2009. The precision of remote context memories does not require the hippocampus. Nat Neurosci 12:253–255.

Warner-Schmidt JL, Madsen TM, Duman RS. 2008. Electroconvulsive seizure restores neurogenesis and hippocampus-dependent fear memory after disruption by irradiation. Eur J Neurosci 27:1485–1493.

Winocur G, Wojtowicz JM, Sekeres M, Snyder JS, Wang S. 2006. Inhibition of neurogenesis interferes with hippocampus-dependent memory function. Hippocampus 16:296–304.

Worley PF, Bhat RV, Baraban JM, Erickson CA, McNaughton BL, et al. 1993. Thresholds for synaptic activation of transcription factors in hippocampus: Correlation with long-term enhancement. J Neurosci 13:4776–4786.

Zhao C, Teng EM, Summers RG Jr, Ming GL, Gage FH. 2006. Distinct morphological stages of dentate granule neuron maturation in the adult mouse hippocampus. J Neurosci 26(1):3–11.

Zhao C, Deng W, Gage FH. 2008. Mechanisms and functional implications of adult neurogenesis. Cell 132:645–660.